Trans Indian Inst Met (2015) 68(2):219–228
DOI 10.1007/s12666-014-0447-y

TECHNICAL PAPER

TP 2847

Optimum Process Parameters for Enhanced Uniform Hardness Distribution and Barreling Behavior in Upsetting

Ch. HariKrishna · M. J. Davidson · Ch. Nagaraju

Received: 11 September 2013 / Accepted: 17 July 2014 / Published online: 29 October 2014
© The Indian Institute of Metals - IIM 2014

Abstract The present work focuses on the application of 'Taguchi' optimization technique for the upsetting of AA2014 cylindrical billets. Different height (h) to the diameter (d) ratios, different lubricants, and billets aged to different times were considered as process parameters. The experimental results proved that the hardness is not uniform throughout the entire billet and will vary with the lubricant employed at the die/billet interface, height to the diameter ratios and ageing condition. The process parameters were optimized to get uniform distribution of hardness in the billet, to reduce the deformation load and barreling effect. Using ANNOVA analysis, the percentage contribution of each factor was determined. To test the accuracy of the predicted results, confirmation experimental runs were conducted and the results were validated.

Keywords AA2014 · Upsetting · Hardness distribution · Deformation load · Barrel radius · Taguchi approach

1 Introduction

Upsetting being the primary technique to form the material has gained importance in the manufacturing industry. It is a well known fact that the increase in the level of deformation increases the hardness of the material. The hardness is not uniform and will vary inside the billet at different points because of the barreling nature of the billet. The investigation on hardness distribution has become vital and the researchers started working on several bulk deformation processes such as forging, rolling and extrusion. Sonmez et al. [1] carried out finite element studies to produce a cold formed part and developed an analytical equation relating hardness measurement and yield stress. They validated the numerically obtained equation for predicting hardness number with the experimental data available from the bibliography. Haluk et al. [2] worked on cold forging process and established a relation between hardness and effective strain. To achieve better quality of the product, they optimized the die design and preform size by developing Nelder-Mead search algorithm. The hardness distribution was determined using the analytical equation proposed from cold forging process. The results were found to be effective when the developed algorithm was correlated with the finite element model.

Muller et al. [3–5] performed multistage roll forming process on sheet metals to manufacture V-clamps. They developed a relation between plastic strain and micro hardness for the AISI 304 material. The V-clamp roll forming operation was also performed using finite element simulations. The strain near the bend portion of the V-clamp was predicted and the value of the micro hardness was evaluated using the relation developed. The micro hardness values obtained from the experimentation was in close proximity with the values of the micro hardness obtained from the numerical equation. Paralikas et al. [6, 7] investigated the consequences of chief process parameters in rolling operation on the quality of V-section geometry. They focused on the prediction of longitudinal and shear strains using finite element simulations. Their continuous effort to optimize the process parameters improved the quality of the formed product by minimizing the longitudinal strains to 20–35 %

Ch. HariKrishna (✉) · Ch. Nagaraju
Department of Mechanical Engineering, V. R. Siddhartha Engineering College, Kanuru 520007, Vijayawada, India
e-mail: harinitw@gmail.com

M. J. Davidson
Department of Mechanical Engineering, National Institute of Technology, Warangal, India

and shear strains to 30–50 %. Lindgren et al. [8, 9] made experimental investigations on the cold rolling of sheet metal to form U-channel. Their mathematical modeling on the stress and strain distributions has laid the foundation of further studies on the forming processes.

Hot working and heat treatment of the material also improves the mechanical properties of the material. Few researchers [10] have worked on the hot working of vanadium micro alloyed forging by considering temperature, strain and cooling rate as parameters. It has been proved that the post mortem billets after increasing the cooling rates increases the hardness, deformation load and ultimate strength. Li et al. [11] performed experiments on aluminium alloys. Forged 7050 aluminum was heat treated to different conditions and with different indentation loads, micro hardness was evaluated for 7050-T77451 and 7050-T7452 billets. They concluded that the heat treatment conditions have shown effect significant effect on the plastic stress–strain relationships and values of hardness and yield strength obtained were in accordance with the results of finite element simulations.

Selvakumar et al. [12–14] conducted workability studies on the powder metallurgy preforms of different height (h) to the diameter (d) ratios. With the variation in the composition and aspect ratio, the change in load required for deformation was investigated. They related the stress and strain parameters with the relative density and analyzed the formability of the material. The micro/meso forming process which undergoes high frequency vibration amplitude assists in improving the softening and hardening of the material. Yao et al. [15] investigated similar kind of studies and their investigation originated the forming process assisted by vibration amplitude. Pradeep et al. [16] carried out experiments on the metal forming process to analyze the surface texture of the harder die surface and the effect of load on the varying friction conditions. With the aid of experimental and finite element simulations, they concluded that the strain rate and flow pattern of the billet are influenced by the friction condition.

The effort to minimize the non-uniform hardness distribution in the billet has not been reported in the bibliography. The objective of the present work is to optimize the process parameters responsible for the non-uniform distribution of the hardness in the billet, barreling behavior and deformation load using Taguchi technique. The optimum process parameters have been suggested and percentage of contribution of each parameter has also been noted down using ANNOVA analysis.

2 Materials and Methods

AA2014 is the material used for the current investigation. The major constituents of this alloying material are Al-0.8Si-4.4Cu-0.8Mn-0.4 Mg. This is one of the most widely used wrought aluminum-copper alloys. This is a heat-treatable alloy and has the behavior of corrosion resistance. AA2014 has the ultimate tensile strength of 483 MPa, yield strength of 414 MPa, Rockwell hardness (RHN-B) of 82 and percentage elongation of 13 %. This alloy is used for heavy-duty forgings, air craft fittings and truck frames.

A 100 ton hydraulic press was used to carry out the upsetting tests. Three sets of cylindrical billets of different height (h) to the diameter (d) ratios namely h/d = 0.5, 0.75 and 1 were placed in between two rigid dies. The diameter (d) of the billet is fixed to 24 mm and the height of the billet is 24 mm for h/d = 1, 18 mm for h/d = 0.75 and 12 mm for h/d = 0.5. Extreme care was taken to place the billets at the center of the die and the ram speed was maintained at 0.5 mm/s throughout the experiments. Nine billets of different aspect ratios were heat treated to a temperature of 502 °C and solutionized in water. To improve the ductility, the billets were heat treated in furnace to a temperature of 160 °C and then aged for 2, 4 and 6 h. Different lubricants namely grease, boric acid and Vaseline were applied on the die/billet interface and were reduced to 30 % as illustrated in Fig. 1. To evaluate the friction factor (m) for the lubricants applied, standard Ring compression test was conducted and the 'm' values for the soap, boric acid, vaseline and un lubricated conditions were obtained as 0.24, 0.33, 0.4 and 0.54 respectively.These lubricants can be used as alternates of conventional lubricants such as molykote, grease and graphite used for metal forming operations. Rao et al. [18] studied the performance of boric acid as lubricant on the surface roughness of the sheets and suggested that boric acid can be used as an alternate to the molykote and grease. To minimize the impacts of the environment; soap and vaseline were used by Narayanan et al. [19] and Mandic et al. [20] in the metal forging operations.

2.1 Finite Element Modeling

Before going to the actual upsetting tests by considering the ageing time, size of the billet and lubrication, the points

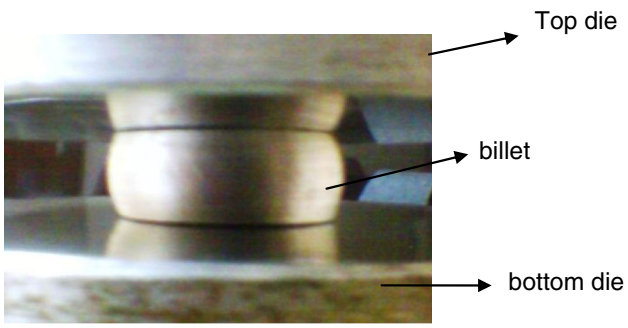

Fig. 1 Billet deformed in between two rigid dies

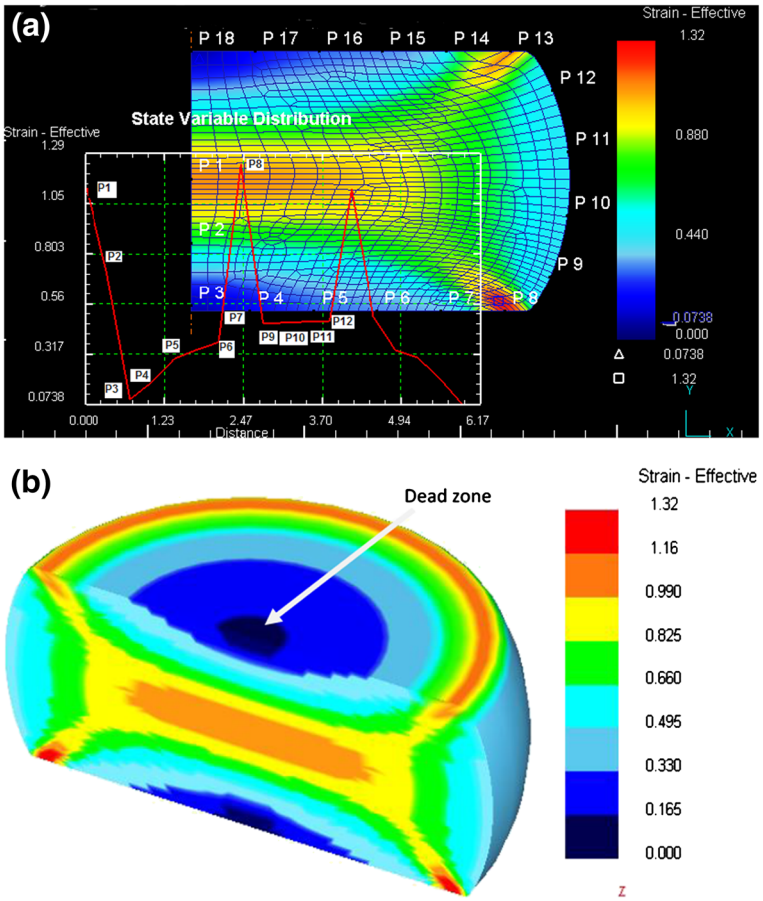

Fig. 2 **a** Strain measurement at different points inside the billet. **b** Depiction of high strained and low strained regions in the billet

of minimum and maximum hardness distribution of the upset billets must be identified. Many authors [19, 21] developed a direct linear relationship between the effective strain and the hardness of the material for bulk forming operations involving radial flow of material. It was proved that the increase in the effective strain increases the hardness of the material. To reduce the extent of experimentation, simulation studies were conducted for the un lubricated condition by considering the fraction factor m = 0.54 at the die/billet interface. The flow stress Eq. (1) was given as input to the finite element software and the billet was reduced to 30 %.

$$\sigma = K\varepsilon^{n} = 720\varepsilon^{0.22} \quad (1)$$

where 'σ' is the flow stress, 'ε' is the true strain; 'K' is the strain hardening coefficient or strength coefficient and 'n' is the strain hardening exponent of the material. The points P1, P2, P3……..P18 in the Fig. 2a, b indicate the values of the strain distributions on the billet and their corresponding values can also be examined on the plot of distance vs. strain effective. The strain distribution is maximum (1.29) at the outer end of the top and bottom surfaces (P8, P13) and minimum (0) near the top surface center (P3, P18). The strain distribution on the periphery (P9–P12) is varying in the range of 0.37–0.44. As per the investigation done by Narayanan et al. [19] the hardness should be maximum at points 'P8' and 'P1', minimum at P3 and moderate at the periphery (P9–P12).

The area of minimum strain distribution called as dead zone exists for all the cylindrical billets compressed plastically irrespective of the any value of the friction factor, aspect ratios and heat treatment condition. This is the reason why the hardness at the point (P3 or P18) was not taken as output parameter for minimum hardness. The strain distribution near the bulge head, center of the billet and outer end of the top surface will vary with the friction condition, aspect ratio and heat treatment. The increase in the bulging also results in loosening of the material and the billet will fracture with the crack initiating near the bulge head [22]. Hence the focus of the present investigation is to reduce the indifference in hardness and the condition proposed should suite any billet formed by employing different friction conditions, aspect ratios and heat treatment. The minimum hardness was measured at the bulge head and maximum near the outer end of the top surface of the billet.

To confirm the predicted results obtained from the simulation, the hardness was measured inside the billets by

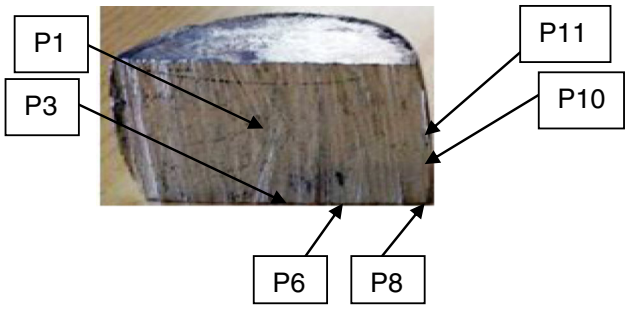

Fig. 3 Measurement of hardness at several points inside the deformed billet

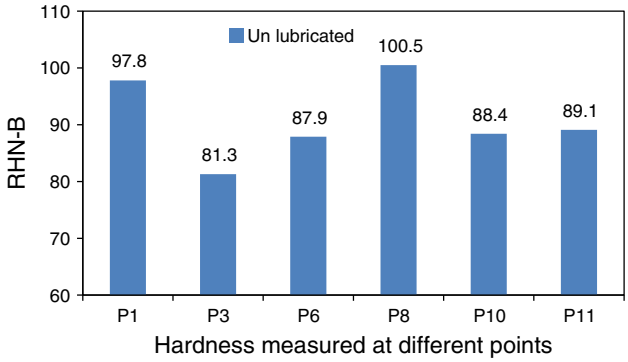

Fig. 4 Values of hardness corresponding the measurements taken in the experiment

cutting it along the axis (Fig. 3). Since the billet is symmetric about X and Y axis quarter portion of the billet was considered and the RHN-B was noted at the points P1, P3, P6, P8, P10 and P11 to obtain the experimental results.

From the illustration of Fig. 4, it can be confirmed that the hardness is maximum near the outer end of the top surface (P8) and minimum hardness was taken at point P10. The experimental results obtained are in accordance with the predicted results and the behavior is in the same way as explained by Narayanan et al. [19]. After determining the zones of maximum and minimum hardness inside the billet, the difference in the maximum and minimum hardness was taken as output parameter and Taguchi technique was applied to optimize the hardness variation for the conditions in Table 1.

For the metal alloy AA2014-T6, $CuAl_2$ is the precipitate. Upsetting makes the plastic flow of these particles to different zones inside the billet. The amount and size of these second phase particles depends on the ageing time causes differential strain hardening. The microstructures of the billets aged for 2, 4 and 6 h are clearly illustrated in Fig. 5. The strength coefficient 'K' will vary which directly reflects the ductility which is in turn responsible for the change in the hardness. The load stroke diagram of the aged billets is illustrated in Fig. 6. The drop in the slope of

Table 1 Factors and levels for the upsetting process

Factors	Factor description	Level 1	Level 2	Level 3
Aspect ratio (h/d)	A	0.5	0.75	1
Ageing time in h (t)	B	2	4	6
Lubricant	C	Soap	Boric acid	Vaseline

the curve indicates the failure point. The billet aged for 2 h has failed earlier than the billet aged for 6 h indicating the difference in the ductility.

The flow stress equations evaluated from the true stress vs. true strain curves (Fig. 7) for the billets aged to 2, 4 and 6 h are represented in Eqs. (2), (3), and (4) respectively. The work hardening coefficients in case of billets aged for 2, 4 and 6 h are 812, 787 and 765 MPa respectively.

$$\sigma = K\varepsilon^{n} = 812\varepsilon^{0.11} \quad (2)$$

$$\sigma = K\varepsilon^{n} = 787\varepsilon^{0.15} \quad (3)$$

$$\sigma = K\varepsilon^{n} = 765\varepsilon^{0.18} \quad (4)$$

3 Analysis of Hardness Variation

The hardness distribution inside the billet is not uniform throughout the entire region of the billet after upsetting because of the barreling nature of the billet. The hardness distribution may vary with the size of the billet, type of lubricant at the die/billet interface and heat treatment. The billets were reduced to 30 % and were cut axisymmetrically to measure hardness at two different points (Fig. 8). To identify the effect of these parameters, Taguchi method was adopted to achieve uniform distribution of the hardness throughout the entire billet, to reduce the load required for deformation and to reduce the barreling nature of the billet. The factors and levels considered for the investigation are listed in the Table 1.

After conducting all the nine experiments, the results were noted down in Table 2. The response 'R1' indicates the difference in the Rockwell hardness-B at the top surface of the billet measured at the center $(RHN\text{-}B)_c$ and at the outer end $(RHN\text{-}B)_e$ is indicated by 'Δ RHN-B'. The barrel radius after deformation was also calculated for all the experiments using the Eq. (1) proposed by Narayanasamy et al. [17] where h_f is the height after deformation of the billet, D_b is the bulged diameter, D_c is the contact diameter and R_a is the barrel radius.

$$R_a = \frac{h_f^2}{4(D_b - D_c)} \quad (5)$$

To obtain the results of minimum deviation in hardness distribution, the response 'smaller the better' has been

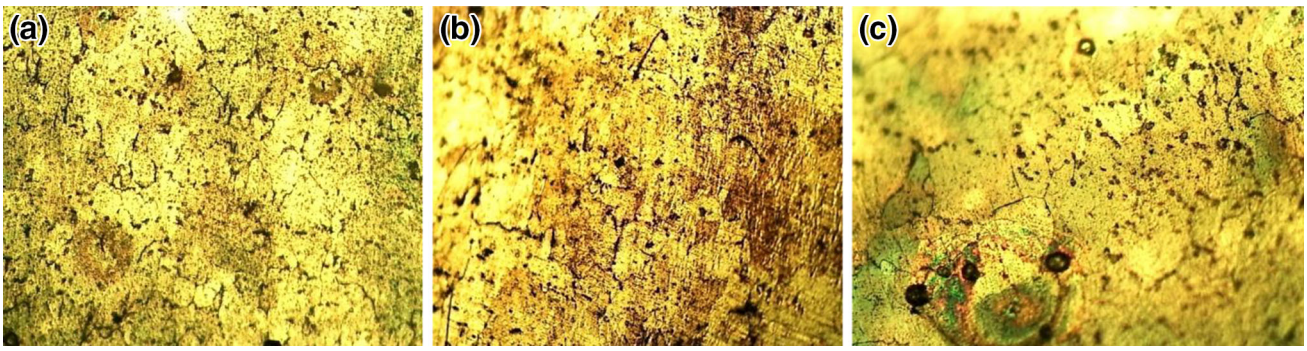

Fig. 5 Microstructures of billets aged for **a** 2 h **b** 4 h **c** 6 h

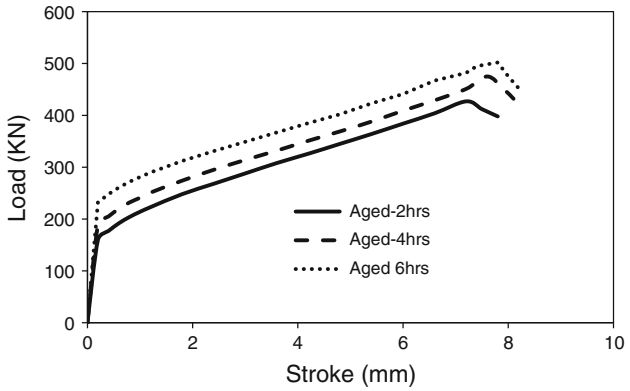

Fig. 6 Load vs. stroke diagram of the aged billets

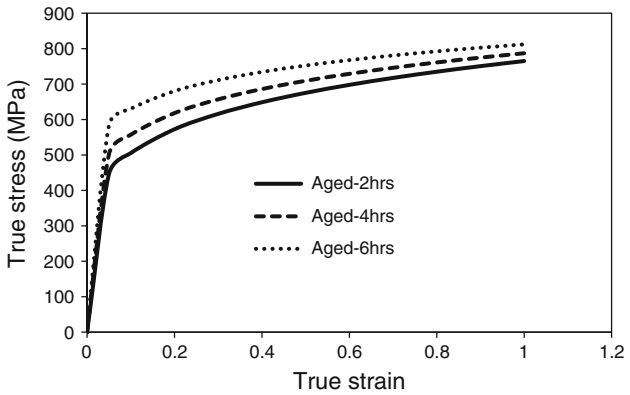

Fig. 7 True stress vs. true strain curves for the aged billets

chosen for which the signal to noise ratio S/N ratio Eq. (2) is as follows

$$\text{S/N ratio} = -10log\left[\frac{1}{n}\sum_{i=1}^{n} Y_i^2\right] \quad (6)$$

where Y_i is the measured value of the response characteristic and 'n' is the no. repetitions for the experimental condition. Signal to noise ratio (S/N) values for different levels and different factors are calculated from the above formula and given in Table 3.

The value of delta presented in the Table 3 explains the ranking position of the process parameters. It is evident that friction is the dominant factor among all the parameters followed by size of the billet and ageing time. The main effects plots for S/N ratio are clearly illustrated in Fig. 9. To obtain the optimum result, a plot between levels of the experiment and mean of S/N ratios was constructed. The optimum condition for the factors and the levels can be presented as A1, B3 and C1. The mean response of the main effects plot of the factors was also considered for the investigation. The values thus obtained from Fig. 10 confirm the results of main effects plot for S/N ratio and gives the same optimum value (A1, B3 and C1). It can reveal from the above results that the friction plays a dominant role in hardness variation. The aspect ratio h/d = 0.5 has less barreling effect compared to h/d = 1 and 0.75. When the billets of different aspect ratios were reduced to same strain level, the amount of bulge at the equator of the billet will be more in case of h/d = 1 compared to other two aspect ratios. This makes the material to get loosened near the equatorial region of the billet causing differential strain hardening at the center and at the equator. To improve the ductility of the material, the solutionized billets were aged. When the billets were aged for 2 h and deformed, the billets were fractured and this made differential strain hardening in the billets compared to other two ageing conditions.

3.1 Analysis of Variance (ANOVA)

ANOVA is a decision making tool which aids in evaluating the most significant factor among all the process parameters. The output quality characteristic is judged based on the variance, F-ratio and percentage contribution ratio and the results are tabulated in Table 4. Using 95 % confidence level, the results obtained from ANOVA are tabulated in Table 4. The F-ratio and percentage contributions reveal that friction has contributed 54.31 % while the ageing time contributed 1.64 % and the size of the billet has contributed to 40.45 %.

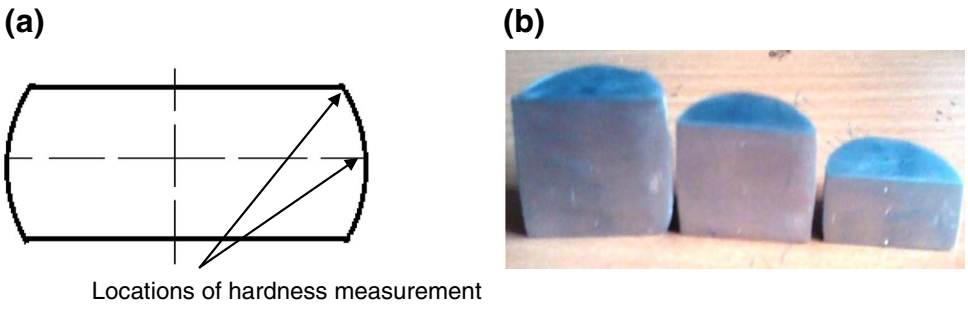

Fig. 8 2D Axisymmetric section of billets **a** Diagrammatic representation **b** Upset billets of h/d = 1, h/d = 0.75 and h/d = 0.5 reduced to 30 %

Table 2 Taguchi L_9 orthogonal array for the experimental design

Experiment no.	Factor A	Factor B	Factor C	$(RHN\text{-}B)_c$	$(RHN\text{-}B)_e$	Response Δ RHN-B (R1)	Barrel radius (R2)	Load (R3)
1	0.5	2	0.24	86.8	93.62	6.82	29.86	464
2	0.5	4	0.33	86	94.62	8.62	22.25	441
3	0.5	6	0.4	86	95.12	9.12	18.17	422
4	0.75	2	0.33	86.5	95.62	9.12	31.509	458
5	0.75	4	0.4	86.5	96.12	9.62	26.92	427
6	0.75	6	0.24	87	94.62	7.62	43.89	390
7	1	2	0.4	86.7	98.12	11.42	33.83	445
8	1	4	0.24	87	96.12	9.12	52.07	404
9	1	6	0.33	87	96.62	9.62	43.08	382

Table 3 Response table for signal to noise ratio (S/N) and means

Response (R1) for signal to noise ratio				Response (R1) for means			
Level	A	B	C	Level	A	B	C
1	−18.19	−18.83	−17.83	1	8.188	9.121	7.854
2	−18.8	−18.97	−19.16	2	8.788	9.121	9.121
3	−20	−19.19	−20	3	10.054	8.788	10.054
Δ	1.81	0.36	2.17	Δ	1.867	0.33	2.2

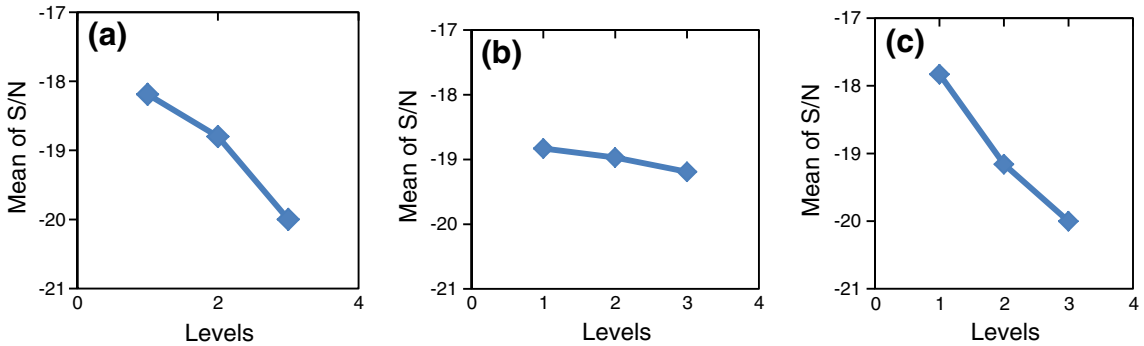

Fig. 9 Main effects plot for S/N ratio to investigate hardness distribution

4 Analysis of Barreling Effect

It is clear from the values of Table 5 that size of the billet is the major factor among all the parameters followed by friction and ageing time. The main effects plots for S/N ratio are clearly illustrated in Fig. 11. The optimum condition for the factors and the levels can be presented as A3, B3 and C1. The factor 'B' has negligible effect on the barrel radius. To explore the quality parameter, the mean response of the main effects plot of the factors was also

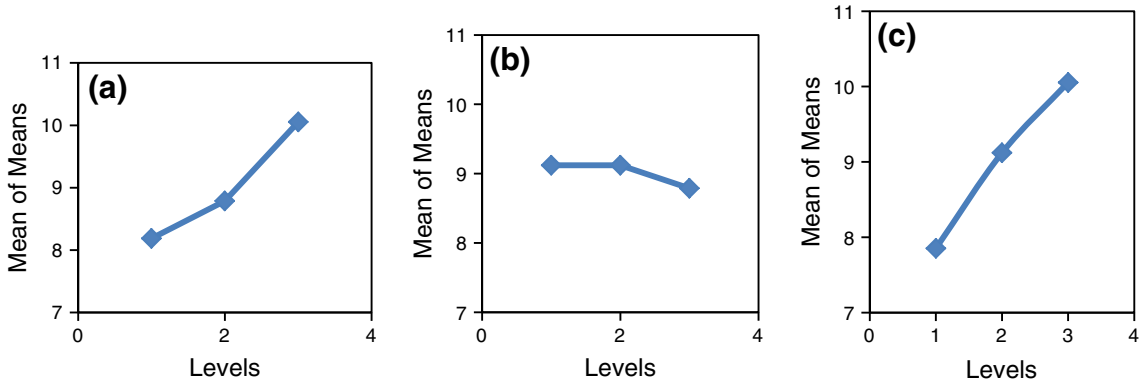

Fig. 10 Main effects plot for Means to investigate hardness distribution

Table 4 Analysis of variance for means

Source	Degree of freedom	Sum of squares	Variance	F-ratio	Contribution ratio (R1) (%)
A	2	5.4489	2.7244	11.30	40.45
B	2	0.222	0.111	0.46	1.64
C	2	7.3156	3.6578	15.17	54.31
% Error	2	0.4822	0.2411		3.58
Total	8	13.468			100

Table 5 Response table for signal to noise ratio (S/N) and means

Response for signal to noise ratio				Response for means			
Level	A	B	C	Level	A	B	C
1	27.21	30.02	32.34	1	23.43	31.73	42.61
2	30.47	30.07	29.87	2	34.11	34.41	32.28
3	32.64	30.24	28.12	3	43.66	35.05	26.31
Δ	5.43	0.22	4.21	Δ	20.23	3.31	16.3
Rank	1	3	2	Rank	1	3	2

considered for the analysis and the results are tabulated in Table 5. The values thus obtained from Fig. 12 corroborate the results of main effects plot for S/N ratio (Fig. 11) and gives the same optimal value (A3, B3 and C1). It can be noted from the above results that the size of the billet plays a leading role in barrel radius. When the billets of different aspect ratios were reduced to same strain level, the amount of bulge at the equator of the billet will be more in case of h/d = 1 compared to other two aspect ratios. This makes the material to get loosened near the equatorial region of the billet causing differential strain hardening at the center and at the equator. To improve the ductility of the material, the solutionized billets were aged. When the billets were aged for 2 h and deformed, the billets were fractured and this made differential strain hardening in the billets compared to other two ageing conditions.

To obtain the results of maximum barrel radius, the response "larger the better" has been chosen for which the S/N ratio Eq. (3) is as follows

$$\text{S/N ratio} = -10log\left[\frac{1}{n}\sum_{i=1}^{n}\frac{1}{Y_i^2}\right] \quad (7)$$

4.1 Analysis of Variance (ANOVA) Barreling

Using 95 % confidence level, the results obtained from ANOVA are tabulated in Table 6. The F-ratio and percentage contributions confirm that size of the billet has

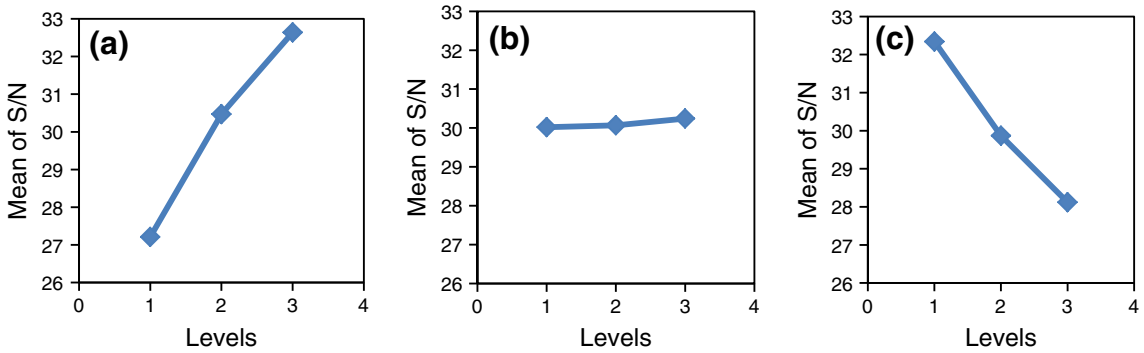

Fig. 11 Main effects plot for S/N ratio to investigate barreling

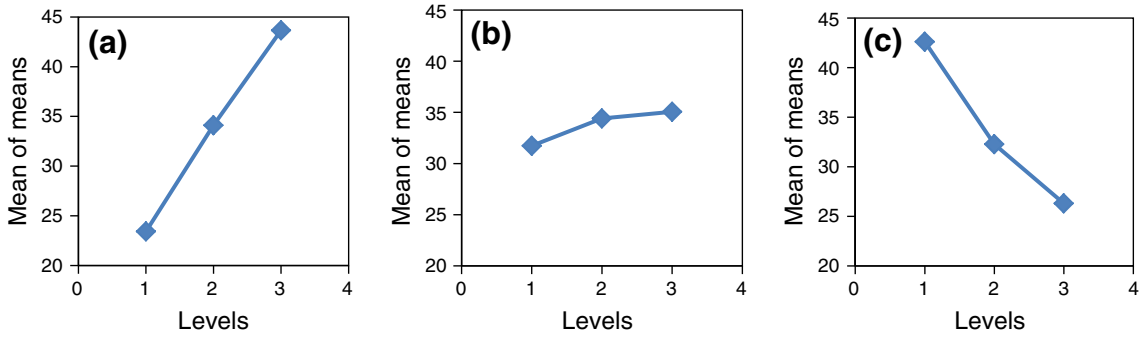

Fig. 12 Main effects plot for Means to investigate barreling

Table 6 Analysis of variance for means (R2)

Source	Degree of freedom	Sum of squares	Variance	F-ratio	Contribution ratio (R1) (%)
A	2	614.72	307.358	188.07	58.84
B	2	18.57	9.283	5.68	1.77
C	2	408.01	204.007	124.83	39.06
% Error	2	3.27	1.634		0.31
Total	8	1044.56			100

Table 7 Response (R2) table for signal to noise ratio and means

Response for signal to noise ratio (S/N)				Response for means			
Level	A	B	C	Level	A	B	C
1	−52.91	−53.17	−52.43	1	442.3	455.7	419.3
2	−52.55	−52.54	−52.58	2	425	424	427
3	−52.25	−51.99	−52.69	3	410.3	398	431.3
Δ	0.69	1.18	0.27	Δ	32	57.7	12
Rank	2	1	3	Rank	2	1	3

contributed 58.84 % while the ageing time contributed 1.77 % and the lubricant at the die/billet interface has contributed to 39.06 %.

5 Analysis of Deformation Load

It is obvious from the values of Table 7 that ageing is the major factor among all the parameters followed by the size of the billet and then lubrication on the deformation load. The main effects plots for S/N ratio are clearly illustrated in Fig. 13. The optimum condition for the factors and the levels can be presented as A3, B3 and C1. The factor 'B' has major effect on the deformation load. To investigate the quality parameter, the mean response of the main effects plot of the factors was also taken into consideration for the study and the results are tabulated in Table 7. The values thus obtained from Fig. 14 substantiate the results of main effects plot for S/N ratio (Fig. 13) and gives the same optimal value (A3, B3 and C1). It can be noted from the above results that the ageing time of the billet plays a leading role in the load required for deformation. The increase in the ageing time improves the ductility of the material. This reduces the load absorption capacity of the billet. Shorter billets absorb more load than the longer billets and this parameter occupies second place among the parameters considered for reducing the load.

5.1 Analysis of Variance (ANOVA) of Deformation Load

A similar procedure has been adopted for investigating the effect of process parameters on deformation load as in the case of studying hardness variation and barrel radius. Using 95 % confidence level, the results obtained from ANOVA are tabulated in Table 8. The F-ratio and percentage contributions explain that ageing time has contributed 73.73 % while the size of the billet has contributed 22.68 % and the lubricant at the die/billet interface contributes to 3.26 %.

5.2 Prediction of Optimum Value for R1, R2 and R2

From the results of S/N ratio and the mean values, the optimum control factors and levels have been chosen as A1, B3 and C1 for R1; A3, B3 and C1 for R2 and R3. The mean optimum values (M_{R1}, M_{R2} and M_{R3}) for the responses can be determined as below

$$M_{R1} = \overline{Y} + (\overline{A1} - \overline{Y}) + (\overline{B3} - \overline{Y}) + (\overline{C1} - \overline{Y}) \quad (4)$$

$$M_{R2} = \overline{Y} + (\overline{A3} - \overline{Y}) + (\overline{B3} - \overline{Y}) + (\overline{C1} - \overline{Y}) \quad (5)$$

$$M_{R3} = \overline{Y} + (\overline{A3} - \overline{Y}) + (\overline{B3} - \overline{Y}) + (\overline{C1} - \overline{Y}) \quad (6)$$

where $\overline{Y}$is the average expansion of all the nine experiments in the Taguchi orthogonal array, A1, B3 and C1; A3, B3 and C1 are the response values of the mean with process parameters at optimum levels. The calculated response

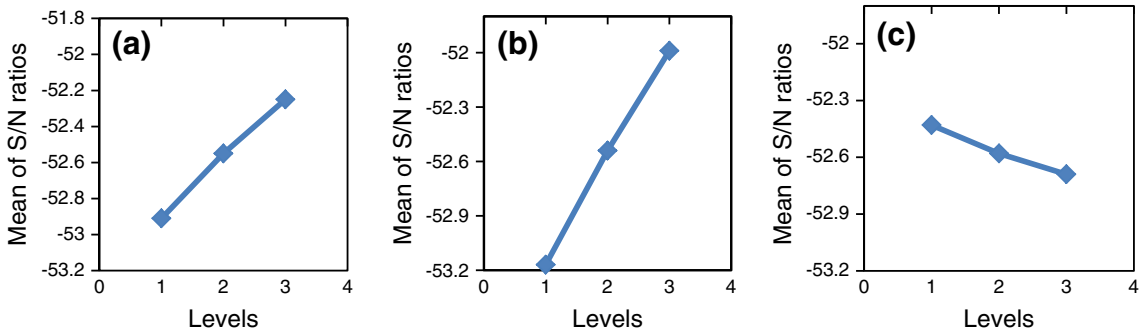

Fig. 13 Main effects plot for S/N ratio to investigate deformation load

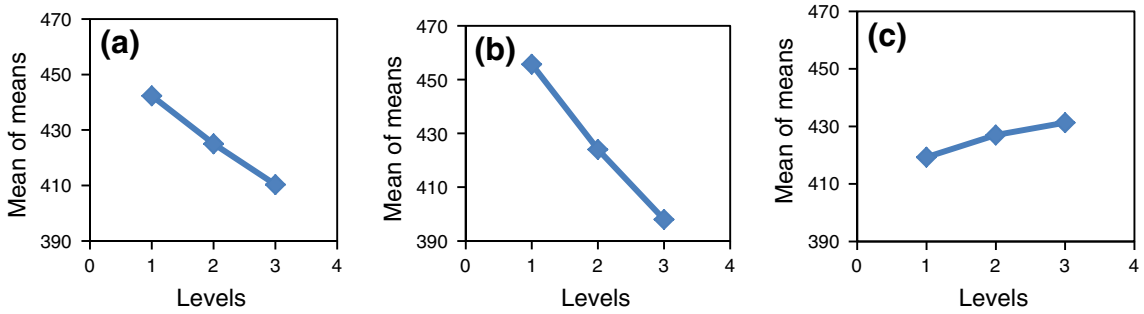

Fig. 14 Main effects plot for Means to investigate deformation load

Table 8 Analysis of variance for means (R3)

Source	Degree of freedom	Sum of squares	Variance	F-ratio	Contribution ratio (R1) (%)
A	2	1539.6	769.78	71.42	22.68
B	2	5004.22	2502.11	232.15	73.73
C	2	221.56	110.78	10.28	3.26
% Error	2	21.56	10.78		0.31
Total	8	6786.89			100

values for M_{R1} is $\overline{Y} = 9.00$, $\overline{A1} = 8.18$, $\overline{B3} = 8.78$ and $\overline{C1} = 7.85$, substituting the values all these factors and the in Eq. 4, the mean optimum value of 'R1' has been predicted as $M_{R1} = 6.82$. The response values for M_{R2} is $\overline{Y} = 33.71$, $A3 = 43.66$, $\overline{B3} = 35.05$ and $\overline{C1} = 42.61$, substituting the values all these factors in Eq. 5, the mean optimum value of 'R2' has been predicted as $M_{R2} = 54.07$. The response values for M_{R3} is $\overline{Y} = 425.88$, $A3 = 410.3$, $\overline{B3} = 398$ and $\overline{C1} = 419.3$, substituting the values of all these factors in Eq. 6, the mean optimum value of 'R3' has been predicted as $M_{R3} = 375.84$.

5.3 Confirmation Run

The confirmation tests were conducted to evaluate the results predicted from Taguchi technique. The predicted results and the experimental results are tabulated in Table 9. It can be examined that the results obtained are within the span of predicted 95 % confidence level and the predicted values are in close agreement with the experimental results.

Table 9 Test data confirmation run

Responses	Optimum factors and levels	Predicted values	Experimental values	Error %
R1	A1, B3, C1	6.82	6.45	5.73
R2	A3, B3, C1	54.07	56.12	3.79
R3	A3, B3, C1	375.84	385	2.44

6 Conclusions

(i) The indifference in the hardness distribution was considerably reduced using the optimization technique. For a material with known properties, the simulation studies helps in optimizing the hardness by predicting the strain distributions.
(ii) The increase in the ageing time has increased the particle size thereby improving the ductility and reducing the hardness of the material.
(iii) The significant factor responsible for the difference in hardness distributions throughout the billet is friction which contributes 54.31 % among the total value.

(iv) The major parameter affecting the barreling behavior is size of the billets which contributes 58.84 % and the ageing condition contributes 73.73 % on the deformation load.

(v) The optimum factors to control the deviation in hardness distribution are A1, B3 and C1; A3, B3 and C1 for barreling behavior and minimum deformation load.

(vi) The optimum value obtained from the Taguchi method is 4.67 for hardness distribution, 54.07 mm for the barreling behavior and 375.84kN for the deformation load.

(vii) The values obtained from the optimum condition of Taguchi method are in good agreement with the confirmation experiments of hardness distribution, barreling behavior and deformation load.

References

1. Sonmez F O, and Ahmet D, J Mater Process Technol 186 (2007) 163.
2. Haluk T, and Sonmez F O, J Mater Process Technol 209 (2009) 1538.
3. Muller M, Barrans S M, and Blunt L, J Mater Process Technol 211 (2011) 627.
4. Muller M, and Barrans S M, in Proceedings of Computing and Engineering Annual Researchers Conference (ED.), University of Huddersfield, Huddersfield, UK (2009) 14.
5. Muller M, and Barrans S M, in 9th International Conference on Turbochargers and Turbocharging, London, UK (2010) 113.
6. Paralikas J, Salonitis K and Chryssolouris G, Int J Adv Manuf Technol 44 (2009) 223.
7. Paralikas J, Salonitis K, and Chryssolouris G, Int J Adv Manuf Technol 47 (2010) 1041.
8. Lindgren M, J Mater Process Technol 186 (2007a) 77.
9. Lindgren M, Ste Res Int 78 (2007b) 82.
10. Babakhani A, Kiani-Rashid A R and Ziaei S M R, Mater Manuf Process 27 (2012) 135.
11. Li J, Li F, Fengmei X, Jun C, and Bo C, Mater Des 37 (2012) 491.
12. Narayanasamy R, Selvakumar N, and Pandey K S, Mater Des 28 (2007) 1358.
13. Mohan-Raj A P and Selvakumar N, Mater Manuf Process 26 (2011) 1388.
14. Sumathi M and Selvakumar N, Mater Manuf Process 26 (2011) 826.
15. Zhehe Y, Gap-yong K, Leann F, Qingze Z, Deqing M and Zichen C, Mater Manuf Process 28 (2013) 584.
16. Pradeep L, Menezes K and Satish V K, Mater Manuf Process 25 (2010) 1030.
17. Narayanasamy R and Pandey K S, J Mater Process Technol 72 (1997) 201.
18. Rao KP and Xie CL, Tribol Int 39 (2006) 663.
19. Narayanan RG, Gopal M and Rajadurai A, J Test Eval 36 (2008) 1.
20. Mandic V and Stefanovic M, Tribol Int 25 (2003) 78.
21. Petruska J and Janicek L, J Mater Process Technol 143-144 (2003) 300.
22. Hari Krishna C, Davidson MJ, Nagaraju C, and Ramesh Kumar P, J Test Eval 43 (2014) 1.